INTERNATIONAL JOURNAL OF CONSERVATION SCIENCE
ISSN: 2067-533X Volume 17, Issue 2, 2026: 529-546 www.ijcs.ro
DOI: 10.36868/IJCS.2026.02.08

INTEGRATED VSM AND FTIR ANALYSIS OF ARCHAEOLOGICAL CERAMICS FOR CONSERVATION PURPOSES

Wassef Al SEKHENEH[1,*], Robert MULLER[2], Miriam Al SEKHANEH[3], Jürgen POPP[2,4]

[1] Department of Conservation and Management of Cultural Resources, Faculty of Archaeology and Anthropology, Yarmouk University, Irbid, Jordan
[2] Leibniz Institute of Photonic Technology (IPHT) in Jena
[3] Karlsruhe Institute of Technology (KIT)
[4] Leibniz Institute of Photonic Technology (IPHT) (Director) in Jena and Chair of Physical Chemistry at Friedrich Schiller University in Jena

Abstract

This study presents a novel investigation into the taxonomy of Jordanian ancient ceramics within an archaeological framework. Pottery fragments dating to approximately 2000 years before the present were analyzed using Vibrating Sample Magnetometry (VSM) and Fourier Transform Infrared Spectroscopy (FTIR), applied here for the first time to such materials. VSM was employed as a quantitative tool to differentiate and group ceramics based on their magnetic properties, while Differential Thermal Analysis and Fourier Transform Infrared Spectroscopy (FTIR) were used to study and examine the relationship between mineralogical composition and magnetic behavior of molecular structure. The integration of these techniques enables a more reliable characterization of ancient ceramic materials and supports informed conservation strategies. The findings highlight the value of advanced, non-destructive analytical approaches in promoting sustainable and compatible preservation of Jordanian archaeological ceramics.

Keywords: *OPTIR, VSM, FTIR; Classification; Pottery; Raman; XRD; Decapolis-Jordan*

Introduction

The primary aims of this research, conducted on very small fragmentary samples from several sites in the Hashemite Kingdom of Jordan, aim to study, specifically, sites in northern Jordan from various cities of the Decapolis, discovered in different periods. The overlap of these periods enriches our understanding of manufacturing methods and the exchange of technical expertise. Strategically selected sites indicate the potential for valuable archaeological discoveries in Jordan, particularly in the northern region and its surroundings, which will enhance our knowledge of Roman-era cities and settlements and their continuation through the Byzantine and Islamic periods. This understanding shapes our comprehension of the synchronicity and overlapping of historical periods that have shaped the region, lending this fascinating interaction a rich historical depth. The imposing ruins of Roman cities in Jordan—the Decapolis cities and those that followed them, as well as the desert fortresses—provide scholars with a wealth of data that helps us understand the relationship between architectural design and urban planning, as well as the study of materials and aspects related to place and time. However, questions remain regarding interpretation and dating, which influence our assessment of the historical trajectory of the region's societies and cultures and their development.

* Corresponding author: sekhaneh@yu.edu.jo

The Decapolis was a group of ten cities in the eastern part of the Roman Empire, renowned for their Hellenistic culture and influence. Most archaeological remains attributed to the Decapolis have been found in the Irbid governorate, particularly in the Plain of Hauran, which extends into southern Syria. This historical context underscores the importance of Yasileh as a site of interest for researchers aiming to deepen their understanding of the Decapolis cities [1-4].

Therefore, this topic and new methods of archaeological measurement were chosen for use at Jordanian sites rich in cultural information, along with efforts to map the geographical distribution and cultural significance of these ancient cities in the Hashemite Kingdom of Jordan. Given the valuable results of excavations in the surrounding areas, many sites from which archaeological samples have been collected offer an opportunity to fill gaps in our historical knowledge of the region. Current findings and future excavation goals at sites like Duhala have focused primarily on uncovering conclusive evidence linking the site of Dion to the network of ten Decapolis cities, most of which are located in northern Jordan [1], [2], [3].

Ongoing excavations are yielding insights into the role of the Decapolis cities across various historical periods, including the Hellenistic, Roman, Byzantine, and Islamic eras.

Each stage of the excavation is crucial in building a critical scientific historical narrative of the Jordanian sites by introducing modern methods through archaeometry and heritage conservation science and highlighting the importance of these sciences within the broader context of understanding the socio-archaeological dimension of the Decapolis cities. This contributes to a deeper understanding of these cities through using modern technologies; future studies are expected to yield more insights, enabling researchers to draw important conclusions and thus enrich our understanding of this pivotal period in Jordan's history. Using these modern scientific methods that shed light on the past to light the present and enlighten the future so that we can see its most obscure aspects. expected to yield further insights, enabling researchers to draw significant conclusions and thus enriching our understanding of this pivotal period in Jordan's history.

The Decapolis was a group of ten cities in the eastern part of the Roman Empire, renowned for their Hellenistic culture and magnificent architecture, which has been preserved for centuries to this day. Numerous archaeological remains from the Decapolis cities have been discovered in the northern governorates of *Irbid*, *Jerash*, and *Ajloun*, particularly in the Hauran Plain, which extends into southern Syria, Lebanon, and Jordan. This ethnographic dimension underscores the Decapolis's importance as a focal point for researchers seeking to deepen their understanding of it and its cultural landscape, moving beyond purely geopolitical interpretations.

The Archaeological Site

The study concentrated on northern Jordan, concerned with sites containing Decapolis remains. The Decapolis, a loose, probably administrative-economic league of ten autonomous Greco-Roman towns, flourished in present northern Jordan, northern Palestine, and southern Syria. Although references to the Decapolis are found in several historical writings, these sources lack consensus as to the number and names of these cities. In the 1st century AD, Pliny names the Decapolis towns as *Damascus*, *Philadelphia*, *Raphana*, *Scythopolis*, *Gadara*, *Hippos*, *Dion*, *Pella*, *Gerasa*, and *Canatha*, while Ptolemy, a century later, not only omits *Raphana* but also names an additional nine towns: *Heliopolis*, *Abila*, *Saana*, *Hina*, *Abila* Lysanias, *Capitolisa*, *Edrei*, *Gadora,* and *Samulis*, making a total of nineteen. Although the writings of Pliny and Ptolemy are the prime resources, scattered references to Decapolis towns can also be found in other historical records.

The study of toponyms and their geographical distribution in conjunction with fieldwork in the Decapolis area has enabled the identification of some Decapolis towns [4] with existing sites. It is now generally accepted that *Scythopolis* is Beisan, Pella is *Tabaqat Fahil*, Philadelphia is Amman, *Gerasa* is *Jerash*, *Gadara* is *Umm Qais*, and *Hippos* is Hippos. Clearly then, further

research is needed to complete the identification of all the Decapolis cities illustrated in the map in figure 1 [10], [11].

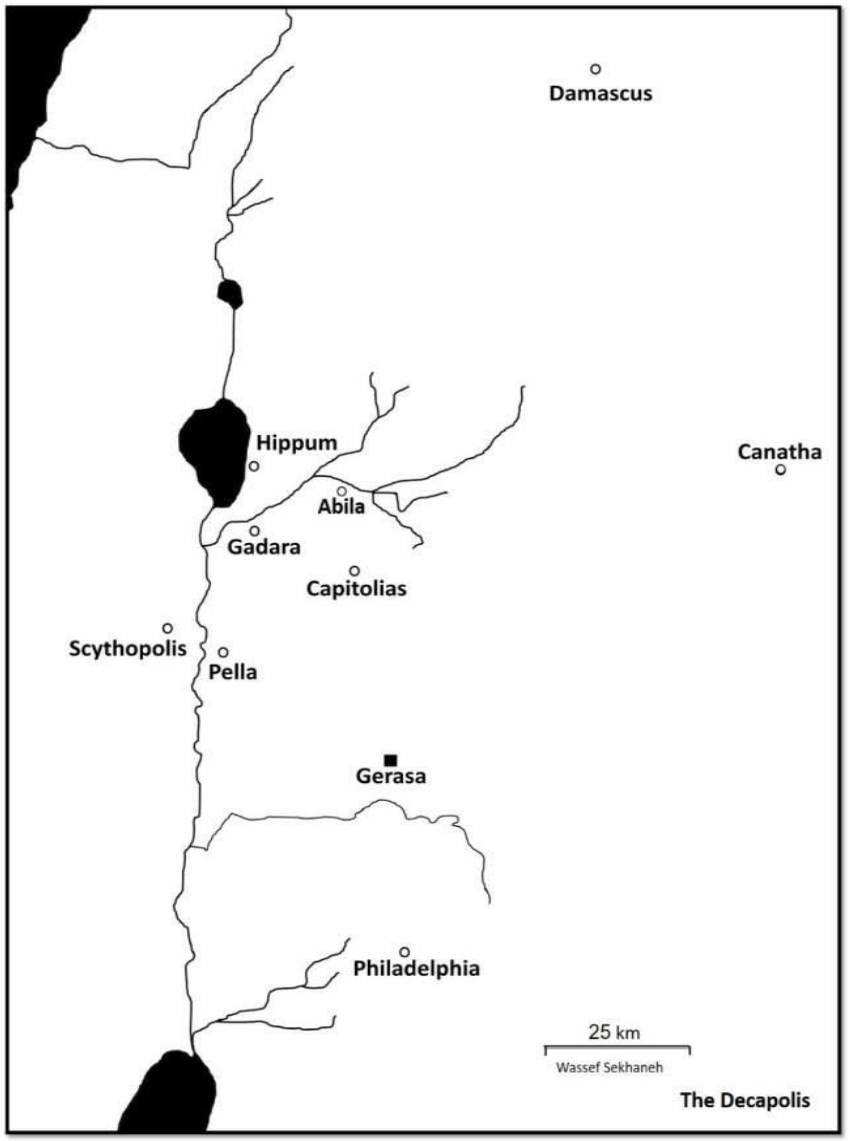

Fig. 1. The map shows the location of pottery sherd sites in northern Jordan and the Decapolis cities' locations. The map revealed Gerasa (Jerash) among them. (Sekhaneh)

Theoretical background of Vibrational Sample Magnetometry (VSM)

This innovative applied research presents an optimal method, using a Vibrational Sample Magnetometer (VSM), for analyzing and classifying archaeological ceramic fragments. This approach represents a new addition to the field of archaeometry, as this method has rarely been used in archaeology. The research primarily aims to classify broken pottery fragments into homogeneous groups based on their magnetic properties, specifically hysteresis curve characteristics. This supports archaeological restoration and facilitates pottery typology for

archaeologists. By identifying similarities among the fragments, it becomes possible to reconstruct complete pottery pieces efficiently and reliably [5], [6].

Magnetic analysis of ceramic samples using magnetic hysteresis was conducted, as most pottery contains iron oxides that exhibit ferromagnetic or ferroantimagnetic behavior, depending on the phase. During this study, a large number of pottery fragments were collected from various Decapolis cities and other locations to develop a classification method. This method aims to facilitate the work of restorers in Jordan and to be disseminated internationally, as it represents the first method of classifying pottery. A preliminary study by the same researchers was accepted and used to prepare samples from archaeological sites in the Hashemite Kingdom of Jordan. The samples used in this study were obtained by cutting pieces of pottery with approximate dimensions of 10×10×8 mm. The findings suggest the need for the increasing integration of archaeomagnetism, specifically methods based on vibratory magnetometry, into archaeological research for dating and classification purposes. These methods can significantly improve our ability to distinguish between pottery assemblages belonging to different production contexts or technical traditions. Therefore, continued multidisciplinary excavation and analysis will be crucial. Future research combining archaeomagnetism, mineralogical analysis, and spatial studies is expected to provide deeper insights into the historical development of the site. The samples used in scanning electron microscopy (SEM) were prepared by breaking off a small piece from each acid-treated sample, taking care to ensure a flat sample surface, and then depositing a thin layer of chromium 10 nanometers thick.

Scanning electron microscope (SEM) images were acquired in the range of 2 to 500 micrometers, using magnifications ranging from 100 to 21,000 times, an acceleration voltage between 8 and 30 kV, and an emission current of 82 μA, operating in both secondary electron (SE) and backscattered electron (BSE) modes. X-ray diffraction (XRD) analyses were performed using an A-45-Cu X-ray tube with a copper (Cu Kα) target, at a high voltage of 40 kV and an anode current of 30 mA. The 2θ angle range used was between 4 and 40 degrees, with a step size of 0.02 degrees and a scanning speed of 2 degrees per minute.

VSM application of Ceramics and Iron Oxides

The magnetic variables and parameters indicated by these physical equations enable us to determine the phase properties of different iron oxides, such as hematite and magnetite, according to their different crystal structures. For example, magnetite exhibits saturation magnetization and magnetic coercivity, while hematite exhibits another magnetization and higher magnetic coercivity. Magmite exhibits intermediate behavior. These factors directly influence the shape of the magnetic hysteresis curve in samples containing iron compounds and provide insight into the firing conditions and microstructure changes of the ceramics. Vibrating Sample Magnetometry (VSM) is a highly innovative technique used to measure the magnetic properties of iron oxide clay materials (iron being ferromagnetic) by observing the resulting magnetic moment under the influence of a strong applied external magnetic field. In this study, VSM was used to analyze archaeological ceramic fragments and extract key magnetic parameters reflecting their composition, varying degrees of firing, and the synergy of these effects with heat-induced chemical transformations. Therefore, it is an innovative technique in the field of clay materials and is used to measure the magnetic properties of materials by monitoring the induced magnetic moment under the influence of an applied external magnetic field. In this study, a VSM method was used to analyze pottery and ceramic fragments and extract the main magnetic parameters that reflect their composition and thermal history [7], [8]. Its use is very rare, and there are pioneers in this field. Therefore, this technique will be of particular importance in archaeology, as the magnetic properties of ceramics are greatly affected by its application. This research will be published later and is particularly relevant in conservation science and archaeological typology, as the magnetic properties of ceramics are strongly influenced by the mineral composition and

firing temperature and conditions; thus, VSM provides indirect but valuable information about ancient production technologies and material sources [9, 10]. VSM utilizes the magnetic properties of ceramic materials containing various iron oxides such as magnetite (Fe_3O_4), hematite (Fe_2O_3), and maghemite (γ-Fe_2O_3). The magnetic behavior of the ceramics is highly dependent on the firing temperature, particle size, and phase composition; these factors control the transformation and distribution of iron minerals within the ceramic materials [11], [12], [13]. Magnetic moment (m) and magnetization (M) are the main parameters in VSM analysis and are related by $m = M \cdot V$ and $M = m/V$. In ceramic systems, the concentration and type of iron oxides present principally regulate the magnetization. Higher magnetite content leading to higher magnetic moment and magnetization values. The relationship between magnetic induction (B), applied magnetic field (H), and magnetization is given by the equation $B = \mu_0(H + M)$. In ceramic, the magnetization is much smaller than the applied field ($M \ll H$), except for samples that have rich ferromagnetic phases. Saturation magnetization (M_s), well-defined as the value of magnetization at high applied external fields, attends to give information about the composition of the artifacts. Magnetite is characterized by high M_s values; however, hematite shows very low saturation magnetization. Remanent magnetization (M_r), measured at zero applied field, provides magnetic stability, where high values indicate stable magnetic domains and low values or superparamagnetic behavior [10], [14]. Saturated magnetization (M_s), defined as the limiting value of magnetization in a strong external magnetic field, provides insight into the crystalline structure of a sample. Magnetite exhibits high M_s values, while hematite shows low saturated magnetization. Residual magnetization (M_r), measured when the external magnetic field is removed, indicates weak or strong magnetic behavior [14], [15].

The coercive field (Hc), defined as the field applied to reduce magnetization to zero, is a key factor. Hematite typically exhibits high coercivity, reflecting strong magnetic behavior, while magnetite shows low coercivity, resulting in weak magnetic properties. These properties determine the mineral phases and firing conditions of archaeological pottery and help estimate the particle size that constitutes the artifact [16]. Magnetic susceptibility (χ), stated as $\chi = \frac{dM}{dH}$or approximately by $\chi \approx \frac{M}{H}$, gives a measure of the material's response to an external applied magnetic field. High susceptibility values are related to ferrimagnetic phases; however, low values agree with weakly magnetic materials. Hysteresis analysis further embodies magnetic performance, where the energy loss is given by $W = \oint H\, dM$. A wide loop specifies hard magnetic behavior, while a narrow loop reflects soft magnetic properties [17, 18]. Analysis using first-order reflection curves (FORC) allows a detailed study of magnetic interactions and grain size distributions. The FORC distribution is defined as follows:

$$\rho(H, H_r) = -\frac{1}{2}\frac{\partial^2 m(H,H_r)}{\partial H\, \partial H_r}, \qquad (1)$$

lets separation of magnetic components and interactions. Through coordinate transformation, the coercive fields are stated as $H_c = \frac{H-H_r}{2}$and $H_i = -\frac{H+H_r}{2}$, respectively, if that requires more information about particle size distribution and magnetic interactions with materials. α-hematite (α-Fe_2O_3) characterizes an important phase in archaeological ceramics. It is the most stable and commonly happening phase type of hematite and exhibits a crystal structure. Magnetically, α-hematite is antiferromagnetic but displays weak ferromagnetism due to its spin canting [19], [20], [21]. The hysteresis behavior of α-hematite is characterized by very low saturation magnetization (M_s), low remanent magnetization (M_r), and high coercivity (Hc). The low M_r, defined as $M_r = M(H = 0)$, specifies weak magnetic properties and arises from the slight canting of antiparallel spins. In contrast, the relatively high coercive field, well-defined by $M(H_c) = 0$, reflects a strong resistance to magnetization reversal. This parameter is highly sensitive to microstructural factors such as particle size, crystallographic defects, and firing, making it particularly appreciated for

interpreting technological conditions in ceramic [21, 22]. Vibrating Sample Magnetometry (VSM) is widely employed to investigate the magnetic properties of ceramic materials, particularly those containing iron oxide phases such as hematite (Fe_2O_3), magnetite (Fe_3O_4), and maghemite (γ-Fe_2O_3). The magnetic behavior of ceramics is strongly influenced by firing temperature, particle size, and phases, which all control the distribution and transformation of iron-bearing minerals within the ceramic objects.

This mathematical relationship, the law of approach to saturation:

$$M(H) = M_S\left(1-\frac{a}{H}-\frac{b}{H^2}\right), \qquad (2)$$

is used to evaluate the magnetic anisotropy and measure the microstructural properties of the studied material characteristics. Furthermore, the internal magnetic field, specified by this equation $H_{\text{int}} = H_{\text{applied}} - NM$, gives the highlights of sample geometry. Shape-related demagnetization properties must be corrected for accurate measurements [23], [24].

Hysteresis Loop Analysis

Hysteresis Analysis, Magnetic Classification, and Archaeological Implications. The magnetic properties of the samples were evaluated through hysteresis loop analysis, which describes the relationship between magnetization (M) and the applied magnetic field (H). The magnetization is approximated by the equation $M = M_s\tanh\left(\frac{H}{H_c}\right)$, reflecting the progressive alignment of magnetic with increasing field strength. The hysteresis loop delivers several parameters that are essential for magnetic characterization. These include the coercive field (Hc), as a field required to reduce magnetization to zero; the remanent magnetization (M_r), representing the remanent magnetization after removal of the applied field; and the saturation magnetization (M_s), corresponding to the maximum magnetization achieved under a strong magnetic field [25, 26]. The analysis demonstrated that pottery samples can be systematically grouped according to their magnetic signatures. In some cases, the magnetization behavior can be described by an exponential model, $M(H) = M_{max}(1 - e^{-kH}) - M_{min}$, which reflects a gradual magnetization process controlled by internal structure and mineral composition. The firing process plays a critical role in modifying the magnetic properties of ceramic materials. Firing of pottery treatment induces transformations in iron oxides, leading to measurable changes in magnetization. These variations can be expressed as

$$\Delta M_s = M_s^{initial} - M_s^{fired} \text{and } \Delta M = M^{initial} - M^{fired}. \qquad (3)$$

These changes are associated with the evolution of superparamagnetic particles and phase transitions within iron oxides. From an archaeological perspective, the integration of VSM into ceramic analysis provides a powerful and non-destructive tool for interpretation [27], [28]. Magnetic classification enables the identification of fragments belonging to the same artifact, facilitates the distinction between locally produced and imported ceramics, and provides insights into manufacturing technologies and firing conditions. Furthermore, this approach supports reconstruction and conservation efforts by offering a scientifically grounded method for grouping ceramic sherds. Overall, the application of VSM represents a significant advancement in archaeometry, offering new perspectives on the study of ceramic materials. Its continued use is expected to yield deeper insights into the cultural, technological, and economic aspects of ancient societies, particularly within the Decapolis region [27].

Materials and Analytical Approach

A total of fifteen pottery samples collected from various archaeological sites at northern Jordan were analyzed using VSM. Each sample was cleaned and prepared to ensure accurate magnetic measurements. The magnetization response of each specimen was recorded under varying magnetic field strengths, generating hysteresis curves for further analysis. Material and

One of the most significant aspects of the ongoing research involves the innovative use of Vibrational Sample Magnetometry (VSM). VSM is a cutting-edge scientific technique that utilizes magnetic properties to analyze materials [19], [20]. In the context of archaeology, it has been employed to categorize and analyze broken pottery pieces discovered at the site. These fragments, often overlooked in traditional archaeological practices, can provide invaluable insights into the daily life, trade, and cultural practices of the people who inhabited the Decapolis.

Hence the importance of this study, which focuses on the reuse of a new technique in preserving and restoring archaeological pottery to keep it alive for as long as possible and to get more information about the art of ceramic production. Three samples of Roman pottery (samples 1, 2, and 3) were collected from the site shown in figure 2.

Fig. 2. Pottery in the Site of Yasileh

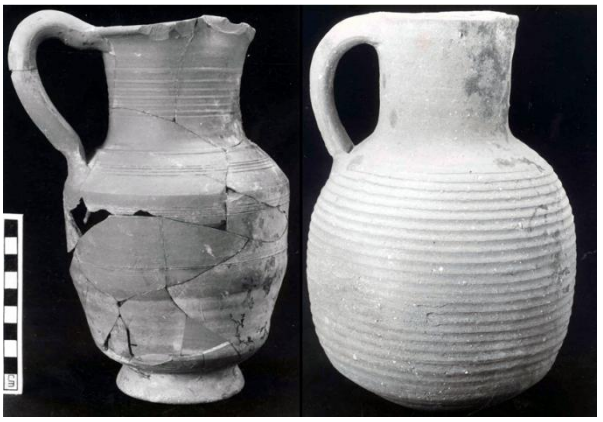

Fig. 3. Cooking pot (Al Muheisen)

A complete cooking pot with a diameter of 3.12 cm is shown in figure 3. Broad everted rim with two loop handles attached from the rim to the shoulders. Omphalos-rounded base. Redware (7.5YR 5/6 Red) with fine-sized white and black grits. Smooth surface covered with red slip on both sides. Sharply close ribbing covered all exterior surface.

Complete jug with a diameter of 3 cm in figure 4. The inverted rim has a spot and groove to receive a lid, with one loop handle attached to the rim and to the shoulder, which has a ridge on the exterior side. Ring base. Light red fine ware (7.5TR 6/8 light red) with very fine-sized

white and black grits. The surface treatment is covered with light red slip on both sides. Slightly close ribbing covered the upper exterior part's surface.

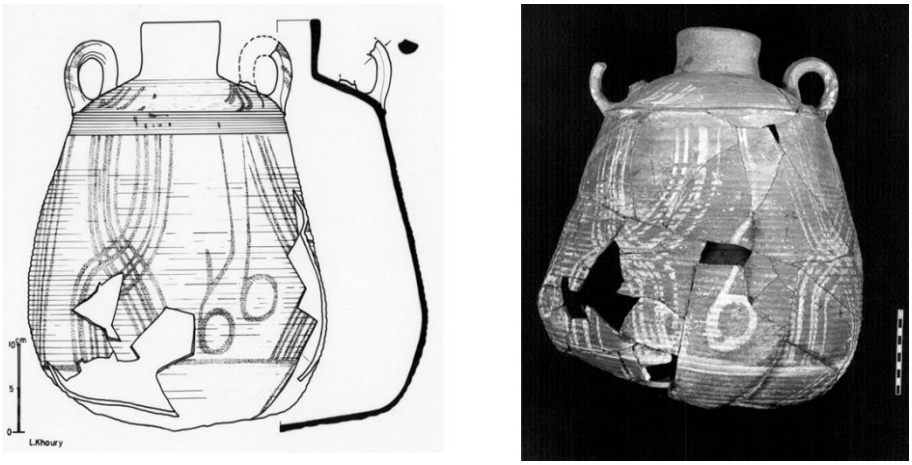

Fig. 4. Jug (Al Muheisen)

Evaluation of Magnetic Properties in Archaeological Pottery Samples

In this study, we analyzed fifteen different pottery samples using a Vibrating Sample Magnetometer (VSM) to investigate their magnetic behaviors through the examination of hysteresis curves. The shape of the hysteresis loop is crucial for understanding the magnetic properties of these archaeological ceramic samples, as it provides insight into their coercivity and remanent magnetization [29], [30]. Magnetic investigations, although widely applied in geology, remain underutilized in the study of archaeological ceramics. Conventional techniques such as X-ray diffraction (XRD) and thermal analysis (DTA/TG) provide valuable mineralogical information; however, their effectiveness is limited in ceramic systems due to low concentrations of iron-bearing phases, overlapping diffraction peaks, and the unknown nature of original raw materials and firing conditions. As observed in this study, quartz was identified as the dominant phase, while minor phases such as calcite and akermanite were detected. Nevertheless, the identification of magnetic iron oxides (e.g., magnetite and maghemite) remained inconclusive using these methods alone [31]. Thermal analysis revealed only minor transformations, with weak exothermic effects and negligible mass changes, which could not be definitively linked to specific mineral phases. These findings confirm that XRD and DTA/TG, when used independently, are insufficient for the reliable classification of ceramic samples [31-34].

In contrast, Vibrating Sample Magnetometry (VSM) proved to be a more sensitive and effective technique for characterizing ceramic materials. The magnetization curves reflect contributions from ferrimagnetic, paramagnetic, and diamagnetic components, enabling a more comprehensive understanding of the samples. Variations in magnetic behavior are strongly influenced by firing conditions, particularly changes in the Fe^{2+}/Fe^{3+} ratio, which affect the formation and transformation of iron oxides. Although parameters such as coercivity (Hc) and remanence ratio (M_r/M_s) provide useful insights, they are not sufficient for classification in systems with mixed magnetic phases. Instead, the overall shape of the hysteresis loop offers a more reliable basis for distinguishing between samples. These results demonstrate that VSM is a powerful complementary tool that overcomes the limitations of conventional analytical methods. Its application enables improved differentiation and grouping of ceramic materials, providing valuable insights into their composition, firing conditions, and technological history.

Hysteresis Loop Analysis

The hysteresis loop is a graphical representation of the relationship between magnetization (M) and the applied magnetic field (H). The key parameters obtained from the hysteresis loop include: Coercivity (H_a): The magnetic field strength at which the magnetization of the sample becomes zero after saturation. Remanent Magnetization (M_r): The magnetization left in the sample when the external magnetic field is removed. Saturation Magnetization (M_s): The maximum magnetization achieved at high magnetic fields. The general equation that describes the hysteresis loop can be expressed as:

$$M = M_s \cdot \tanh(H / H_a) \quad (5)$$

where H_a is the applied magnetic field strength. The analysis of the hysteresis loop allows us to categorize the pottery samples based on their coercive behaviors. Classification of Pottery Samples. Our findings revealed that the pottery samples could be grouped based on their coercive characteristics. Notably, one sample, which was broken into three pieces, exhibited similar magnetic properties across the fragments. This similarity is characterized by low coercivity and a quasi-inverse magnetization curve, as illustrated in the following equation:

$$M(H) = M_{max} \cdot (1 - e^{\wedge}(-kH)) - M_{min} \quad (6)$$

where k is a constant that describes the steepness of the curve. The decrease in specific magnetization (M_s) and overall magnetization compared to the corresponding clay sample indicates a gradual change in the mixture of magnetic minerals due to the firing process.

Impact of Firing on Magnetic Properties. The observed magnetic properties are primarily influenced by the content of superparamagnetic iron oxide particles within the pottery samples. As the clay is subjected to increasing temperatures during the firing process, the transformation of magnetic minerals occurs, leading to the following changes:

$$\text{Decrease in Specific Magnetization: } \Delta M_s = M_s^{(initial)} - M_s^{(fired)} \quad (7)$$

$$\text{Decrease in Overall Magnetization: } \Delta M = M^{(initial)} - M^{(fired)} \quad (8)$$

These equations illustrate the significant reduction in magnetization as a result of the thermal treatment of the clay samples. The Implications for Archaeological Analysis The differences in magnetic properties among the pottery samples allow us to evaluate the firing processes and material components utilized in their production. By identifying specific magnetic characteristics, we can create classifications of pottery types that share similar qualities. This classification process is essential for restorers and archaeologists, as it aids in the reconstruction of fragmented pottery objects [35], [36].

Results and Discussion

XRD and DTA/TGA Analysis

Magnetic investigations are well known in geology to characterize the remanent magnetization of rocks, whereas only a few publications are available dealing with magnetic properties of (ancient) ceramics [beat]. Such properties might be useful for a distinction or classification of ceramics. Usually, iron impurities in the raw materials form magnetic phases whose amount is quite low, which leads to problems in their identification by X-ray diffraction (XRD). The value of differential thermal analysis/thermogravimetry (DTA/TG) investigations on fired ceramics is limited as well since there are influences from the initial composition of the raw material and from the firing conditions that are not known. Investigations with methods like electron microscopy (incl. EDX, etc.) might be too expensive or time-consuming, but we haven't done it. A first indication of different preparation conditions or compositions is given by the color of a new fracture surface corresponding with the typical different colors of iron oxide compounds. However, only dominant compounds can be distinguished: Fe^{3+} - compounds are usually red (hematite γ-Fe_2O_3) or beige-orange (maghemite α-Fe_2O_3). With increasing Fe^{2+} content, the materials become

darker. Magnetite (Fe_3O_4) is black. Compared to iron, the amount of other heavy metal impurities is usually negligible. A first characterization of the samples was done by XRD (Figs. 5 and 6) and DTA/TG. X-ray diffraction investigations were used to characterize the different phases of the ceramics (X'Pert PRO, PANalytical, The Netherlands). In all cases the major phase is quartz. Other important (non-magnetic) phases that could be determined are calcite (samples 13, 14, and 16) and akermanite (sample 12). Not all phases could be identified. The ferrimagnetic maghemite seems to be in samples 12, 14, 15, and 18. A distinction between maghemite and magnetite is not possible in our samples. Both materials have a spinel structure. The amount is small, though the detection is not very clear, particularly since hematite was found as well in the samples (not in sample 12) whose peak positions superimpose partly on the magnetite peak positions. Some of the samples (11, 12, 14, and 15) were investigated by differential thermal analysis/thermogravimetry (DTA/TG) (NETZSCH-Gerätebau GmbH, Selb, Germany) under air with a heating rate of 5 K/min, a maximum temperature of about 1060°C, and a subsequent cooling with 10 K/min to room temperature. DTA/TG shouldn't reveal an irreversible reaction under conditions (T, atmosphere) similar to the firing conditions. After firing under oxidizing conditions, there shouldn't be an indication of a decomposition of organic material or water at lower temperatures (<500°C) if there is no alteration. Under reducing firing conditions, remaining carbon (from organics) could decompose (oxidation) during the measurement. A possible magnetic phase could be magnetite (Fe_3O_4) (or an intermediate phase α-Fe_2O_3–Fe_3O_4) that oxidizes into Fe_2O_3.

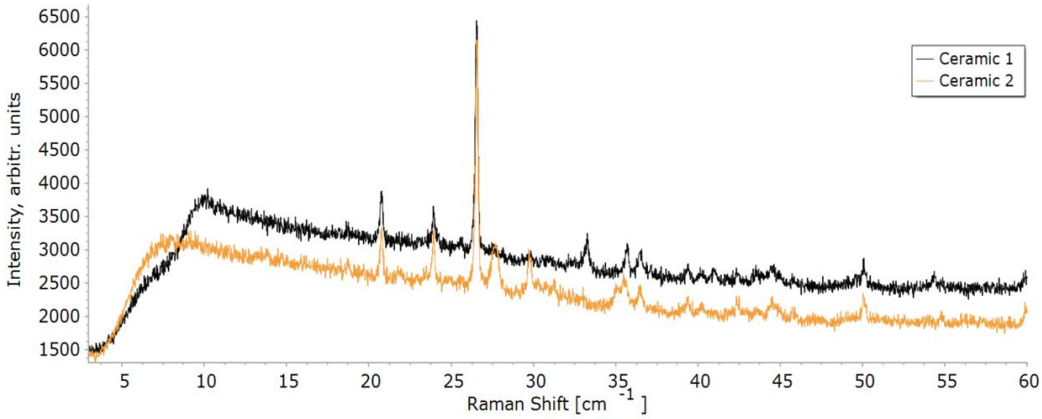

Fig. 5. Shows an example of an XRD pattern

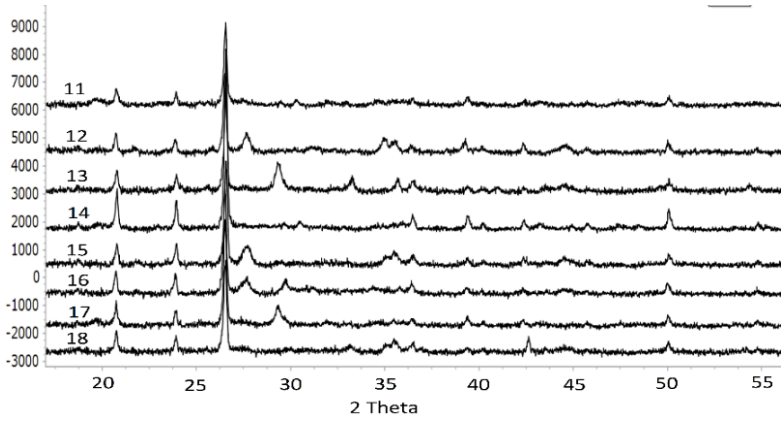

Fig. 6. Shows an example of an XRD pattern of the ceramic samples

The magnetization loop MV(H) (M: magnetization, V: sample volume (constant), H: magnetic field strength) of the samples was measured within about 15 min. All measurements were normalized to the sample mass. The specific saturation magnetization values of the samples, taken from the magnetization loops, are a material constant of a ferro- or ferrimagnetic phase or allow estimating the amount of a (known) magnetic phase in the sample, assuming a certain specific saturation magnetization of the phase, e.g., Fe: 217 Am^2/kg, Fe_3O_4: 90 Am^2/kg [LB], α-Fe_2O_3: ≈ 65 Am^2/kg [LB], or γ-Fe_2O_3: 15 Am^2/kg [Jin]. The values can deviate for nanoparticle samples or by deviations in the oxidation state of Fe (forming a solid solution γ-Fe_2O_3–Fe_3O_4) [4]. This effect can be superimposed by a linear M(H) behavior of para- or antiferromagnetic (small positive slope, e.g., α-Fe_2O_3, Fe-salts, Fe-hydroxides, and Fe-oxyhydrates; most Co- and Ni-compounds; natural clay minerals) or diamagnetic materials (very small negative slope, e.g., H_2O, quartz, and most organics), both usually called "non-magnetic" materials. If Fe ions are incorporated into the lattice of silicates, which are theoretically diamagnetic, they may become paramagnetic. Considerable differences in the magnetic behavior of ceramics may occur even if the same initial materials (clay, etc.) were used if different firing conditions change the Fe^{2+}/Fe^{3+} redox conditions. Because of the firing or a possible alteration in the course of time, Fe as a magnetic phase can be excluded. The magnetization data of samples were corrected by the diamagnetic effect of the sample holder and container.

The coercivity Hc of a magnetic material (x-axis intercept of the magnetization curve) depends on the magnetocrystalline anisotropy constant K of a material (i.e., on the crystal structure) and the particle size and shape. K can be influenced by impurities or dopants in the crystal lattice. The influence of the size dominates near the transition size from superparamagnetic (SP) to stable ferro/ferrimagnetism (about 10 nm). SP particles have an Hc=0; magnetically stable magnetite particles show an Hc in the order of 10 kA/m.

The remanence ratio M_r/M_s shows a dependence on the particle size similar to that of Hc. However, the parameters differ in case of samples consisting of a mixture of magnetic phases (or different demagnetization mechanisms). For geological samples, often the remanent magnetization is important. Because of the different superimposing influences, Hc and M_r/M_s only seem to be not ideal parameters for a classification, but the shape of the magnetization curve gives information about mixed magnetic phases.

Different types of magnetization curves of the samples can be distinguished. F: ferrimagnetic (or ferromagnetic, not superparamagnetic), e.g., γ-Fe_2O_3, Fe_3O_4, ferro: Fe F+P: ferri- + paramagnetic(-like) superposition, P: Fe-salts, Fe-hydroxides, α-Fe_2O_3, most Co- and Ni-compounds) F+E: ferrimagnetic + a hard magnetic behavior known from ε-Fe_2O_3. Magnetization corresponds with the amount of magnetic phase (correct only if one phase. Type F: coercivity depends on particle size and shape and doping ($Fe_{3-x}MexO_4$). Relative error < 5%; low signal of samples 11 and 13, values less accurate are shown in table 1.

Table 1. Magnetic Properties of Samples

Sample	Specif. Magnetization (Am^2/kg)	Coercivity (kA/m)		Type
11	0.09	19.5	F+P	terracotta
12	0.79	13.4	F	grau
13	0.13	7.2	F(+P)	hell orange
14	0.48	17.9	F+E	tc
15	2.1	30.0	F	dark braun
16	0.27	9.4	F+E	gray brown
17	0.36	23.2	F	tc
18	1.45	10.8	F	braun

Figure 7 shows the magnetization loops of ceramics with a superposition of a "magnetite-like" phase with a hard magnetic phase (samples 14 and 16, type F+E) and a para- or antiferromagnetic phase (samples 11 and 13, type F+P), respectively.

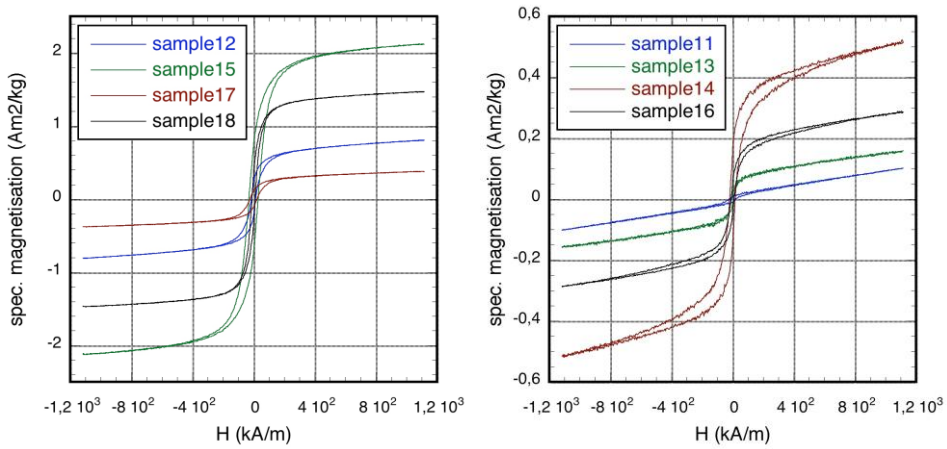

Fig. 7. Magnetization loops of ceramics containing phases with ferrimagnetic behavior (type F) typical for magnetite/maghemite or spinel ferrites.

The DTA curves of samples in figure 8, samples 11, 12, 14, and 15 reveal a small exothermic peak at about 650°C connected with a mass loss of about 1.5 wt% (samples 12 and 14). The decomposition temperature of calcite is usually given as >800°C. So we are not sure what phase originates the mass loss. The transformation between α and β-quartz at 573 °C couldn't be seen, although quartz is the major phase. The amount of iron oxide estimated from the magnetic data is too low to detect a possible oxidation of Fe_3O_4 by thermogravimetry. There are no DTA peaks in the cooling curves, which indicates an irreversible reaction, which means the firing doesn't lead to this reaction. Summarizing, we have to notice that both XRD investigations and DTA/TG investigations are not sufficient to classify the samples. Static magnetic measurements were used to characterize and to distinguish different types of ceramics. The measurements were performed on a Vibrating Sample Magnetometer MicroMag™ 3900 (Princeton Measurements Corp., USA) at room temperature. The ceramic samples were crushed into pieces of some 10 mg weight, and one piece was measured in each case.

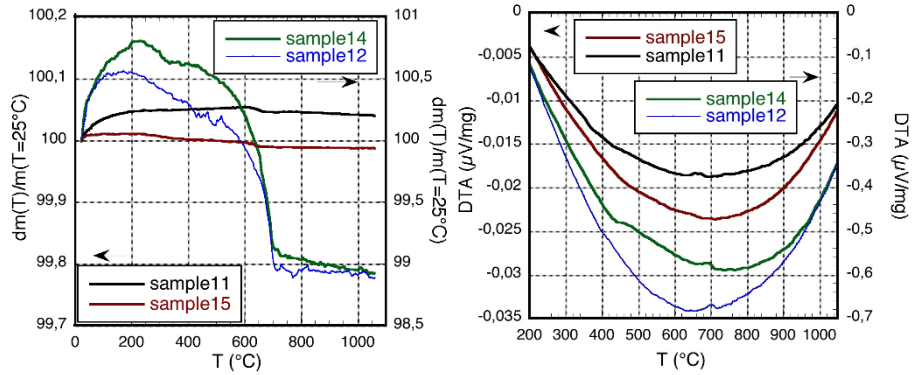

Fig. 8. Shows the DTA pattern of the pottery samples 11, 12, 14, 15

This article presents infrared spectroscopy, X-ray diffraction, and VSM analysis of Nabataean and Roman pottery sherds from various sites in Jordan. These sherds may be from complete pieces that were broken by accident in ancient times, and this study is undertaken to investigate the conservation and preservation purposes. The pottery paste was used to produce high-quality pottery objects, known as eggshell pottery because of their very low thickness, made from heavily crushed clay mixed with very fine desert sand, adding some organic materials and coloring

the surfaces from the outside to give the artifact a warm color and protect it from environmental degradation. We also highlight the so far unknown pleasant smell of this material and the many uses of Nabataean pottery, from the clean and wastewater pipes in the drinking water supply networks to the sanitation of the unfit water that flows into the city of Petra, Jordan.

Undoubtedly, one of the most important aspects of the study of the VSM to investigate the ferromagnetic properties of ceramics is to determine the preferred direction of study in the field of cultural heritage conservation. Ferromagnetic properties of ceramic are to determine the preferred direction of study in the field of cultural heritage conservation. Generally, to answer this question, microstructural studies have been carried out, including X-ray diffraction analysis, which can be lengthy processes if we take into account the sample preparation for each type of analysis and the nature and reasons for performing this type of experiment. However, the magnetic measurement of the clay pieces in parallel and perpendicular directions allows us to give a quick answer to this question, namely the classification of ceramics into groups for conservation. Therefore, thermal studies were also useful in this case, since at temperatures above 830°C in air some chemical transformations occur, such as the conversion of calcium carbonate to calcium oxide.

The samples were subjected to X-ray diffraction (XRD) analysis using a Philips X'Pert diffractometer with Cu Ka radiation. The diffractograms were subsequently analyzed utilizing the X'Pert HighScore software, together with the PCPDFWIN database (2002 JCPDS). Consequently, the crystal size was calculated based on line broadening of the diffraction patterns through implementation of Scherrer's equation. The quasistatic magnetic characterization of the pottery sherds was conducted via vibrating sample magnetometry (VSM; MicroMag TM3900, Princeton Measurement Corporation, Princeton, Westerville, OH, USA). The magnetic properties were evaluated with a maximum applied field of 12 kW and at room temperature. A calibration curve was constructed using a nickel sphere as the standard reference material. The magnetic hysteresis cycle of pottery pieces was measured using two different magnetic fields: a high intensity of 12 kOe (955 kA/m) and a much lower field of 500 Oe (40 kA/m). The high-intensity field was used to evaluate the saturation magnetization, with the measurement conducted in laboratories at the University of Jena in Germany. The quasistatic magnetic properties were investigated using a MicroMagTM3900 (Princeton Measurements Corp., Westerville, OH, USA) vibrating sample magnetometer (VSM). Hysteresis loops at saturation field strength and a maximum field of 15.4 kA/m, as used in the case of SAR and remanence curve measurements, were determined. The switching field distribution S(H) was calculated from the remanence data using the following equation, with M_r being the field-dependent initial remanence and M_rS as the saturation remanence.

$$S(H) = \frac{dM_r(H)}{M_{rS} \times dH} \quad (9)$$

Increasing the firing temperature up to 820°C leads to the transformation of calcium carbonate in pottery to calcium oxide, which can be identified by X-ray diffraction analysis, as well as kaolinite, which is found in some samples fired at temperatures below 600°C, and the presence of illite decreases. The presence of muscovite decreases as the temperature rises to 850°C and disappears above this value. Montmorillonite, which was present on samples burnt under 600°C and disappears above 820°C. Quartz is present in all samples.

ATR-FTIR Spectroscopy

The ATR-FTIR spectra of the ceramic samples shown in the figures in this study are presented as shown in figure 9; the spectrum of Sample 1 contains a broad band located at 3700–3100 cm^{-1} (centered at 3430 cm^{-1}), as well as a band at 1630 cm^{-1}. These two bands correspond to the ν(O–H) stretching vibrations of water molecules (H_2O) adsorbed on the pottery surface and to the H–O–H bending (δ) vibration of water resulting from the powders' exposure to atmospheric air, respectively. The broad absorption band at approximately 1085 cm^{-1} can be attributed to the stretching vibrations of the Si–O bond, and this may be related to the presence of a quartz phase. The spectrum of the sample is very similar to the previous spectrum, except that it shows an

additional, weak absorption peak at 1381 cm^{-1}. This peak is characteristic of the stretching vibrations (ν_3) of the carbonate ion and is likely attributable to the calcite phase. Based on the FTIR analysis results, it can therefore be concluded that the main chemical composition of the samples is identical, given the high similarity of their spectra. On the other hand, the spectra of some samples contain peaks attributed to C–O vibrations in the carbonate ion. The bands observed at 3450, 1750, 1630, 1085, and 796 cm^{-1} indicate that their chemical composition is very close to that of the carbonate ion. The characteristic bands of the stretching vibrations of the CO_3^{2-} ion appear at 1465 cm^{-1} and 1383 cm^{-1}. The observed splitting of the carbonate peak (ν_3) in the spectrum may indicate the presence of two different phases, such as calcite and aragonite, in the ceramic material. A strong and sharp carbonyl band was observed at 1750 cm^{-1}.

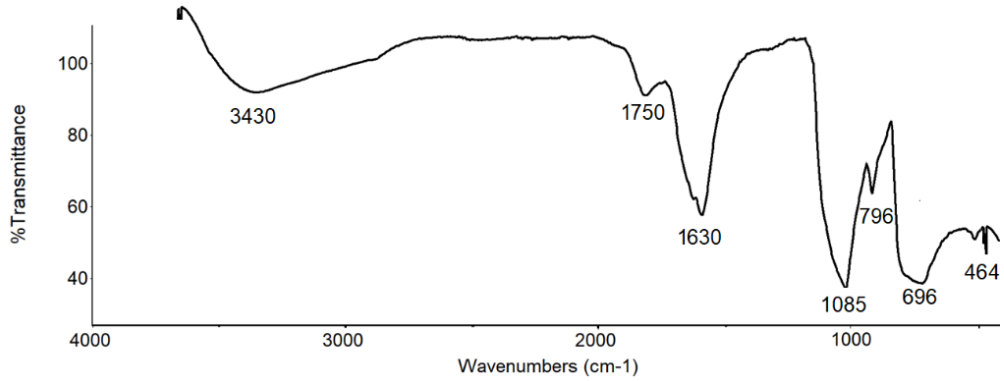

Fig. 9. FTIR Spectrum of the pottery sample

The spectrum of sample No. 2 (Fig. 9) contains the same bands centered at 3435 cm^{-1} and 1637 cm^{-1}, which are attributed to O–H vibrations, in addition to a broad band at approximately 1080 cm^{-1} associated with Si–O vibrations. Several strong bands were also observed in the 1000–600 cm^{-1} region (800, 795, 710 cm^{-1}), which are characteristic of metal–oxygen (M–O) bond vibrations in the ceramic sample.

Optical Photothermal infrared (OPTIR)

OPTIR spectroscopy is a modern technique that combines the advantages of infrared (IR) spectroscopy and optical microscopy (Fig. 10). Simply put, this technique enables scientists to identify and map chemical composition at the nanoscale, something that conventional infrared spectroscopy cannot achieve [37], [38]. OPTIR works indirectly by first heating the sample slightly with an infrared laser.

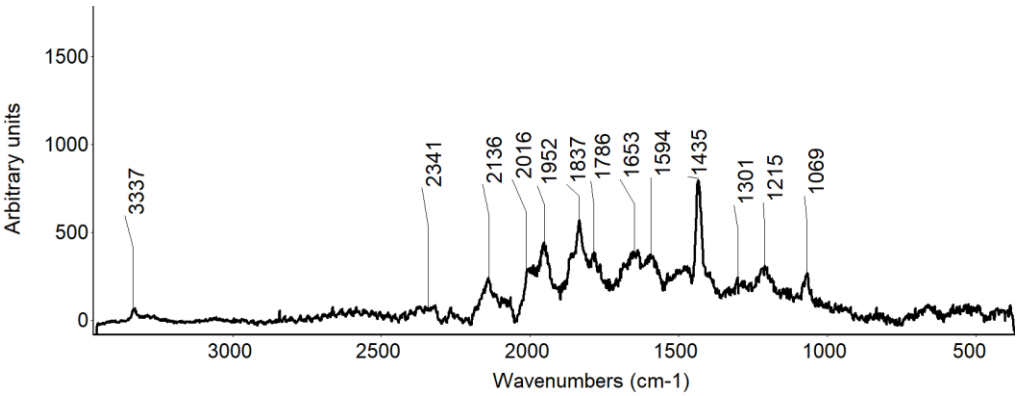

Fig. 10. OPTIR spectrum spectroscopy

This is because molecules absorb infrared light at specific wavelengths, causing minute localized temperature changes. Then, a visible laser detects this thermal effect by measuring the sample's expansion or deformation. This indirect detection is the key innovation behind the technique [39]. OPTIR is highly advantageous because it overcomes one of the major limitations of conventional infrared spectroscopy: providing high spatial resolution and enabling analysis beyond the diffraction limit of infrared light. This technique can be applied to a wide range of materials, and here it has been applied for the first time to archaeological materials, including fine clay particles. Its main advantages lie in combining the chemical specificity offered by infrared spectroscopy and high-resolution optical imaging, its non-destructive nature, and its ability to analyze samples that are difficult to analyze using conventional infrared methods. Conventional infrared spectroscopy has low spatial resolution and relies on direct infrared absorption, while Raman spectroscopy offers higher resolution through light scattering. OPTIR spectroscopy achieves very high resolution by using infrared heating combined with optical detection. In short, OPTIR spectroscopy is a hybrid technology that combines infrared heating and optical detection for high-resolution chemical analysis [40], [41].

Conclusion

This research essentially aims to enhance understanding of the historical role of the Decapolis cities across multiple settlement periods, including the Hellenistic, Roman, Byzantine, and Islamic eras, through the study, classification, and restoration of pottery artifacts. This study demonstrates that applying vibratory magnetometry (VSM) to archaeological pottery represents a valuable methodological advancement in archaeology. Analyzing the magnetic signatures of ceramic fragments provides an innovative and efficient approach to classifying pottery pieces, supporting reconstruction efforts and the interpretive analysis of fragmented materials. In this context, VSM offers a complementary tool to traditional analytical techniques, particularly when dealing with highly fragmented or visually indistinguishable ceramics for restoration, allowing for the individual collection of fragments for the conservator to assemble as a single piece. The results also indicate that the magnetic properties of ancient pottery are not only useful for classification purposes but also provide indirect information about production techniques, including firing temperature, atmospheric conditions, and heat treatment duration. In this study, combining magnetic hysteresis curve analysis with complementary observations, such as color variation, allowed for a more accurate characterization of pottery groups and their potential technical differences. Ultimately, the integration of advanced scientific techniques into archaeological practice not only enhances artifact interpretation but also contributes to a more comprehensive understanding of cultural and historical dynamics in northern Jordan, thereby enriching the broader narrative of the Decapolis region.

Acknowledgments

The researchers are grateful to Prof. Z. Al Muheisen for providing us with the archaeological samples and for valuable discussions. Also, the researchers are grateful to Friedrich-Schiller University in Germany for hosting the research. The researchers would like to sincerely thank Yarmouk University. I am truly grateful for this opportunity from Prof. Jürgen Popp, the Director of the Leibniz Institute of Photonic Technology (IPHT) and the Chair of Physical Chemistry at Friedrich-Schiller-University in Jena, Germany.

References

[1] M. Nassar and Z. Al-Muheisen, "Geometric Mosaic Pavements of Yasileh in Jordan," *Palestine Exploration Quarterly,* vol. 142, no. 3, pp. 182-198, 2010. https://doi.org/10.1179/003103210X12789453090129

[2] Z. Al-Muheisen, "Water Engineering and Irrigation System of the Nabataeans: A Regional Vision," Water Systems at Yasileh," *ADAJ*, vol. 51, pp. 471-486, 2007.

[3] W. Al Sekhaneh, Z. Al-Muheisen, and N. Gharaibeh, "Vibrational Spectroscopy Study of Ancient Bones from Archaeological Sites in Jordan," *International Journal of Conservation Science*, vol. 11, no. 3, 2020, pp. 647-656.

[4] A. Thakur, A. Kumar, and E. Berdimurodov, "Recent Trends in the Synthesis of Multifunctional Magnetic Nanoparticles," *Multifunctional Magnetic Nanoparticles in Therapy, Biology, and Pharmacy*: CRC Press, 2024, pp. 59-91.

[5] T. Salaoru, F. Matau, S. Tascu, L. Curecheriu, and A. Stancu, "Effect of thermal treatment on the magnetic properties of ceramic samples from eastern Romania clay deposits," *Digest Journal of Nanomaterials and Biostructures*, vol. 8, no. 1, pp. 335-346m 2013.

[6] G. R. Annamalaia, R. Ravisankarb, and A. Chandrasekaranc, "Magnetic, Mossbauer and Micro-Analytical Findings of Archaeological Pottery Sample of Manaveli, India," *International Journal of Scientific Research and Engineering Development*, Vol. 2, no. 3, pp. 531-537, 2019.

[7] F. Matau, V. Nica, P. Postolache, I. Ursachi, V. Cotiugă, and A. Stancu, "Physical study of the Cucuteni pottery technology," *Journal of Archaeological Science*, vol. 40, no. 2, pp. 914-925, 2013. https://doi.org/10.1016/j.jas.2012.08.021.

[8] I. Pratikakis, M. Spagnuolo, T. Theoharis, and R. Veltkamp, *A 3D Pottery Content Based Retrieval Method*, PhD Thesis, University (?), City (?), Country (?), 2009.

[9] M. Mandal and D. Sarkar, "Manufacturing Excellence in Ceramic Industry," in *Ceramic Processing*: CRC Press, pp. 1-36, 2019.

[10] S. Abdel-Hameed, M. Hessien, and M. J. C. I. Azooz, "Preparation and characterization of some ferromagnetic glass–ceramics contains high quantity of magnetite," *Ceramics International*, vol. 35, no. 4, pp. 1539-1544, 2009. https://doi.org/10.1016/j.ceramint.2008.08.021.

[11] R. Pullar, W. Hajjaji, J. Amaral, M. Seabra, J. J. W. Labrincha, and B. Valorization, "Magnetic properties of ferrite ceramics made from wastes," *Waste and Biomass Valorization*, vol. 5, no. 1, pp. 133-138, 2014. https://doi.org/10.1007/s12649-013-9207-1.

[12] T. G. Avancini, M. T. Souza, A. P. N. de Oliveira, S. Arcaro, and A. Alves, "Magnetic properties of magnetite-based nano-glass-ceramics obtained from a Fe-rich scale and borosilicate glass wastes," *Ceramics International*, vol. 45, no. 4, pp. 4360-4367, 2019. https://doi.org/10.1016/j.ceramint.2018.11.111.

[13] J. Jacob, MA, Khadar, and M. Materials, "VSM and Mössbauer study of nanostructured hematite," *Journal of Magnetism and Magnetic Materials*, vol. 322, no. 6, pp. 614-621, 2010. https://doi.org/10.1016/j.jmmm.2009.10.025.

[14] M. Ahmadzadeh, C. Romero, and J. McCloy, "Magnetic analysis of commercial hematite, magnetite, and their mixtures," *AIP Advances* vol. 8, Article Number: 056807, 2018. https://doi.org/10.1063/1.5006474.

[15] F. Bødker, M. F. Hansen, C. B. Koch, K. Lefmann, and S. Mørup, "Magnetic properties of hematite nanoparticles," *Physical Review B*, vol. 61, no. 10, Article Number: 6826, 2000. https://doi.org/10.1103/PhysRevB.61.6826.

[16] D. J. Dunlop and P. S. Letters, "Coercive forces and coercivity spectra of submicron magnetites," *Earth and Planetary Science Letters*, vol. 78, no. 2-3, pp. 288-295, 1986. https://doi.org/10.1016/0012-821X(86)90068-3

[17] F. Heider, A. Zitzelsberger, K. J. P. o. t. E. Fabian, and P. interiors, "Magnetic susceptibility and remanent coercive force in grown magnetite crystals from 0.1 μm to 6 mm," *Physics of the Earth and Planetary Interiors*, vol. 93, no. 3-4, pp. 239-256, 1996. https://doi.org/10.1016/0031-9201(95)03071-9.

[18] D. J. Dunlop, Ö. Özdemir, and R. J. Enkin, "Multidomain and single-domain relations between susceptibility and coercive force," *Physics of the Earth and Planetary Interiors*, vol. 49, no. 3-4, pp. 181-191, 1987. https://doi.org/10.1016/0031-9201(87)90021-5.

[19] A. Stancu, "Characterization of magnetic nanostructures with the first-order reversal curves (forc) diagram technique," in *Magnetic Measurement Techniques for Materials Characterization*: Springer, pp. 605-628, 2021.

[20] B. Dodrill, "Magnetometry and First-Order-Reversal-Curve (FORC) Studies of Nanomagnetic Materials," *Encyclopedia of Nanoscience and Nanotechnology* (ed. Dekker), Taylor & Francis, 2016.

[21] R. Egli, "Magnetic characterization of geologic materials with first-order reversal curves," in *Magnetic measurement techniques for materials characterization*: Springer, pp. 455-604, 2021.

[22] A. M. Hirt, "Iron Oxides: From Nature to Applications," *Magnetic measurements and characterization,* Book Chapter, ETH Zürich, pp. 347-370, 2016. https://doi.org/10.1002/9783527691395.ch15.

[23] A. Wendl, H. Eisenlohr, F. Rucker, C. Duvinage, M. Kleinhans, M. Vojta, and C. Pfleiderer, "Emergence of mesoscale quantum phase transitions in a ferromagnet," *Nature*, vol. 609, no. 7925, pp. 65-70, 2022. DOI: 10.1038/s41586-022-04995-5.

[24] O. Bolle, H. Diot, W. Fransen, and M. D. Higgins, "Central sagging of a giant mafic intrusion: The Ediacaran Sept Îles Layered Intrusion (Québec, Canada)," *Journal of the Geological Society*, vol. 178, no. 1, pp. 2020-029, 2021. DOI: 10.1144/jgs2020-029.

[25] E. A. Jagla, "Hysteresis loops of magnetic thin films with perpendicular anisotropy," *Physical Review B*, vol. 72, no. 9, Article Number: 094406, 2005. DOI: 10.1103/physrevb.72.094406.

[26] L. Corbellini, J. Plathier, C. Lacroix, C. Harnagea, D. Ménard, and A. Pignolet, "Hysteresis loops revisited: An efficient method to analyze ferroic materials," *Journal of Applied Physics*, vol. 120, no. 12, Article Number: 124101, 2016. DOI: 10.1063/1.4963756.

[27] A. Kosterov, E. Sergienko, A. Iosifidi, P. Kharitonskii, and S. Y. Yanson, "Analysis of strong-field hysteresis in high coercivity magnetic minerals," in *Problems of Geocosmos–2018: Proceedings of the XII International Conference and School*, Springer, pp. 127-142, 2019.

[28] Ö. Özdemir and D. J. Dunlop, "Hysteresis and coercivity of hematite," *Journal of Geophysical Research: Solid Earth*, vol. 119, no. 4, pp. 2582-2594, 2014. DOI: 10.1002/2013jb010739.

[29] B. Dodrill and J. R. Lindemuth, "Vibrating sample magnetometry," in *Magnetic measurement techniques for materials characterization*: Springer, pp. 15-37, 2021.

[30] S. Santikulthani, T. Eknapakul, S. Pinitsoontorn, and P. Songsiriritthigul, "Systematic investigation and correction of the magnetic hysteresis obtained by vibrating sample magnetometry," *Journal of Physics: Conference Series*, *IOP Publishing*, vol. 2431, no. 1, Article Number: 012058, 2023. DOI 10.1088/1742-6596/2431/1/012058.

[31] R. Ravisankar, A. Naseerutheen, A. Rajalakshmi, G. R. Annamalai, A. Chandrasekaran, and B. Spectroscopy, "Application of thermogravimetry–differential thermal analysis (TG–DTA) technique to study the ancient potteries from Vellore dist, Tamilnadu, India," vol. 129, pp. 201-208, 2014. https://doi.org/10.1016/j.saa.2014.02.095.

[32] R. Ravisankar, A. Naseerutheen, G. R. Annamalai, and A. Chandrasekaran, "Firing Temperature Analysis of Ancient Potsherds from Odugathur, Vellore Dist., Tamilnadu, India by TG-DTA Technique," 2013.

[33] Z. L. E. Ntah, R. Sobott, B. Fabbri, and K. Bente, "Characterization of some archaeological ceramics and clay samples from Zamala - Far-northern part of Cameroon (West Central Africa)," *Cerâmica*, vol. 63, no. 367, pp. 413-422, 2017. DOI: 10.1590/0366-69132017633672192.
[34] D. Seetha and G. Velraj, "Determination of firing techniques of ancient artifacts by using FT-IR analysis," *Chemical Science Review and Letters*, vol. 2, pp. 456-463, 2014.
[35] J. Svoboda, *Magnetic techniques for the treatment of materials*. Springer Science & Business Media, 2004.
[36] A. Ghasemi, *Magnetic ferrites and related nanocomposites*. Elsevier, 2022.
[37] J. S. Böke, J. Popp, and C. Krafft, "Optical photothermal infrared spectroscopy with simultaneously acquired Raman spectroscopy for two-dimensional microplastic identification," *Scientific Reports*, vol. 12, no. 1, Article Number: 18785, 2022. DOI: 10.1038/s41598-022-23318-2.
[38] E. Farnesi, M. Calvarese, C. Liu, C. Messerschmidt, M. Vafaeinezhad, T. Meyer-Zedler, D. Cialla-May, C. Krafft, J. Ballmaier, O. Guntinas-Lichius, M. Schmitt, and J. Popp, "Advancing cerumen analysis: exploring innovative vibrational spectroscopy techniques with respect to their potential as new point-of-care diagnostic tools," *The Analyst*, vol. 149, no. 22, pp. 5381-5393, 2024. DOI: 10.1039/d4an00868e.
[39] S. Adak, A. T. Raveendran, S. F. El-Mashtoly, J. Popp, and C. Krafft, "Enhancing widefield mid-infrared photothermal microscopy with fluorescence detection for improved contrast and cellular imaging," *European Conferences on Biomedical Optics* vol. 2025, pp. Th3A.1, 2025. DOI: 10.1364/ecbo.2025.th3a. 1.
[40] C. B. Prater, M. Kansiz, and J. Cheng, "A tutorial on optical photothermal infrared (O-PTIR) microscopy," *APL Photonics*, vol. 9, no. 9, Article Number: 091101, 2024. DOI: 10.1063/5.0219983.
[41] E. Reiner, F. Weston, N. Pleshko, and W. Querido, "Application of Optical Photothermal Infrared (O-PTIR) Spectroscopy for Assessment of Bone Composition at the Submicron Scale," *Applied Spectroscopy*, vol. 77, no. 11, pp. 1311-1324, 2023. DOI: 10.1177/00037028231201427.

Received: October 02, 2025
Accepted: April 24, 2026